Designing an Energy-Saving Induction Motor Operating in a Wide Frequency Range

Maria Dems , *Member, IEEE*, and Krzysztof Komeza , *Senior Member, IEEE*

Abstract—**Induction motors are an important consumer of electricity. Among induction motors, speed-regulated induction motors have the greatest energy-saving potential. However, motors operating in a very wide speed range require a completely different approach than motors operating on a single supply frequency. An example of such motors are the drives of industrial washing machines. The article aimed to present how using field-circuit methods, but above all, analytical methods increase the efficiency of such a motor by changing its design. Thanks to the change of the design and the core material, it was possible to obtain the efficiency of the motor for the frequency of 10 and 20 Hz, meeting the requirements of the IE1 efficiency class specified for the frequency of 50 Hz, while for the frequency of 10 Hz it is 17.9% higher than in the currently produced motor, and for 20 Hz—by 11.1%, while for the frequency of 350 Hz the level of efficiency was corresponding to class IE4. The presented considerations may be the basis for such a procedure for other drives with similar properties. Additionally, an important element of the article is the refinement of the analytical method of determining core losses.**

Index Terms—**Analytical models, electrical sheets, energy efficiency, finite-element method, induction motors, magnetic losses, professional washing machines, rotating machine measurements, variable speed drives.**

I. INTRODUCTION

IT IS estimated that electric motors consume, depending on the economic sector, from 30 to even 70% of electricity. About 300 000 000 industrial electric motors are installed, and the amount is increasing by 15% annually [1]. Variable speed motors represent the greatest potential for the energy-saving process [2]. For this reason, it is estimated that they account for 30% to 40% of newly installed motors in the European Union (EU) [3]. Currently, concerning motors operating at mains frequencies, quite stringent requirements regarding their efficiency, defined by efficiency classes, apply. Still, there are no clearly defined requirements for motors operating in a wide

frequency range. There are two main approaches for increasing the efficiency in an electric motor. First approach is to improve the physical design of the motor, and second approach is designing a controller for reducing losses in the electric motor [4], [5]. A broad overview of the methods of describing losses in models of induction machines and control methods allowing for their reduction is presented in the article [6]. Another problem is the reduction of power losses in dynamic states, such as start-up or change of rotational speed. The article is limited only to studying static states and increasing the motor's efficiency through design procedures. A limitation for the use of a more sophisticated control method is the fact of striving to obtain the lowest possible cost of the motor with the controller while obtaining energy savings throughout its operation and achieving efficiency close to the value imposed by the efficiency classes specified for the mains frequency, for the motor of the same rated power. The motor under consideration operates under particular conditions. If usually, the constant power speed ratio parameter does not exceed 3:1, even for drives for electric vehicle systems, then in the case of the tested motor, this value is much higher and amounts to 35:2. For operation at high frequency, core losses, including the so-called additional losses resulting from higher harmonics of the magnetic field caused by the slots in the stator and rotor and the winding distribution around the machine circumference, play an essential role in shaping the motor efficiency. These losses are also described as stray losses (SL). It is commonly accepted that these losses are significant for the balance of losses [7], [8]. It is also proved by the results of measurements [9]. The increase in these losses' significance appears when increasing the frequency and when working in the field weakening range [10] and when the motor's rated power is reduced [11]. Hence, the great importance of these losses for the motor is considered in the article. As stated by the authors of the article [12], the article of these losses began at the beginning of the last century. In [13] and [14], we can find a breakdown of individual loss sources into leakage flux losses, high-frequency losses, pulsation losses, cross-current losses, and surface losses. Generally, the SL determination methods can be divided into methods based on measurements, empirical relations, equivalent circuits, analytical methods, and numerical methods. The works in [15] and [16] can be included in the measurement methods. Empirical relations are an extension of the dependencies given in the standards and their refinement [17], [18]. The equivalent circuit uses additional elements placed in the equivalent circuit to model additional core losses [19], [20]. A fairly commonly used method of calculating losses is FEM time-stepping analysis,

most often combined with the calculation of losses in the post-processing phase [21]–[23]. The works of the authors also use this technique [24]–[29]. Classical analytical methods are also developed, which are attractive because the computation time is many times shorter than when using Finite element method (FEM). Here, one can note solutions based on the winding function approach [30] and simplified dependencies not taking into account saturation [31]. More precise methods presented in [32] are based on previous works [33] and [34]–[37]. Based on extensive experimental research and field-circuit modeling, the authors created an analytical core loss model, improved in this article, which allows the determination of core losses with high accuracy. Although based on similar foundations as in [37]–[39], this solution was based on the measured loss characteristics of the magnetic material in a wide range of induction and frequency and presented in [28]. On the other hand, in [26], a new approach was introduced, consisting in the calculation of additional surface losses in the core, to a greater extent taking into account the current state of saturation and the physics of high-frequency field penetration into the sheeted core, which allows for excellent compliance with the measurement for various core materials. In the article, the method of calculating additional surface losses, given in [26], was refined by correcting the calculation of the depth of penetration of individual field harmonics into the surfaces of the stator and rotor teeth.

The motor powered by an inverter in a wide frequency range requires the introduction of structural changes ensuring high efficiency in the entire operating range.

The first works on the construction of induction motors powered by a converter appeared relatively long ago [40]. In the past, work has mainly focused on adapting the conventional rotor geometry to the needs of an inverter-driven induction machine while keeping other parameters unchanged [41]. The work showed that the increase of the maximum motor torque could be obtained by changing the geometry of the machine slots and the thickness of the air gap, thanks to which the stator and rotor leakage reactance is reduced and a larger rotor slot number than stator slot number is further suggested in to reduce the rotor leakage inductance [42], [43]. In turn, on paper [44], it has been shown that the efficiency is insensitive to small changes in the shape of the slots if its surface remains constant. In the following papers, there are many ideas for increasing efficiency for the inverter powered motors. In [45], a relatively wider and shorter rotor slot topology is preferred to reduce the leakage inductance for higher peak torque. Further [46], it has been proposed to fill only a part of the rotor slot with conductive material, which is difficult to implement for a die-cast aluminum cage. In turn, Li and Klontz [47] suggest reducing the air gap, using closed slots, reducing the slots' opening, and a smaller rotor slot depth resulting in loss reduction. In [48], because the authors suppose that the main source of losses is losses in the upper part of the rotor bar, they propose a deepened rotor slot opening with an asymmetric slot closure shape.

In that work, the authors tried to use the proposed methods to achieve greater motor efficiency, but most of them turned out to be useless. This is mainly due to the motor's basic feature, i.e., operation in a very wide frequency range. Methods that
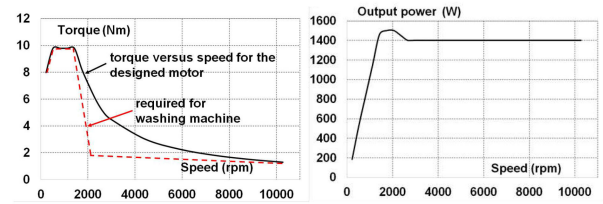
Fig. 1. Comparison of torque versus speed required for washing machine at stationary conditions with the torque obtained for designed motor and output power versus speed for designed motor.

were effective for a single, even high-frequency motor could not be applied because they significantly reduced the machine's efficiency at low frequency. Working in a wide frequency range also means that the motor works in a weakened area for high frequency, which makes it difficult to obtain the required electromagnetic torque. The designed motor was intended for industrial washing machine drives and was a competitive solution concerning other motors used in such drives. Variable frequency drives were first used in industrial washing machines in the mid-1980s. Until then, a system requiring three or four motors and a series of belts, pulleys, jack shafts, and clutches were used to regulate the rotational speed for the wash and spin cycles. Some publications discuss the use of induction motors in industrial washing machines [49]. The article's main aim is to present how to obtain high efficiency and, at the same time, the required electromagnetic torque in a wide range of rotational speeds through the appropriate design of an induction motor. Simultaneously, this motor must meet some design and technological limitations resulting from the washing machine manufacturing process.

II. DESIGNING AN ENERGY-SAVING MOTOR OPERATING IN A WIDE FREQUENCY RANGE

The considered motor for driving industrial washing machines during one washing cycle operates at frequencies of 10 or 20 Hz (starting, soaking of the load and proper washing), and 350 Hz (spinning).

As shown in Fig. 1, they operate at a different value of the electromagnetic torque and have different power on the motor shaft in each of the mentioned frequency ranges. When designing an energy-saving motor for driving industrial washing machines, it was assumed that it would meet at least the requirements of the IE2 efficiency class in the entire operating range, specified for the supply voltage frequency of 50 Hz, while maintaining the overall dimensions imposed by the designers of washing machines. The area provided for mounting the motor in the washing machine limits the maximum outer diameter (the motor is without its own housing) and the motor's overall length. For variable speed drives, the EU Regulation 1781/2019 [50] has recently appeared, which introduces the necessity for motors with a rated power of 0.12 kW or more and equal to or less than 1000 kW to meet the requirements of the IE2 efficiency class (at mains frequency - 50 Hz) [50]. The consequences of these changes are presented in [51]. Table I gives proposed requirements for an exemplary motor's efficiency for driving an industrial washing machine

TABLE I

PROPOSED REQUIREMENTS FOR THE EFFICIENCY OF AN EXEMPLARY
MOTOR FOR DRIVING AN INDUSTRIAL WASHING MACHINE

Supply voltage frequency	Load torque	Output power	Required efficiency at frequency 50 Hz			
Hz	Nm	W	IE1 [%]	IE2 [%]	IE3 [%]	IE4 [%]
10	6.8	170	56.5	64.5	69.5	74.3
20	9.1	500	69.0	76.0	80.0	83.3
50	10.3	1500	77.2	82.8	85.3	88.2
350	1.3	1400	76.7	82.5	85.0	88.0

Fig. 3. Experimental setup.
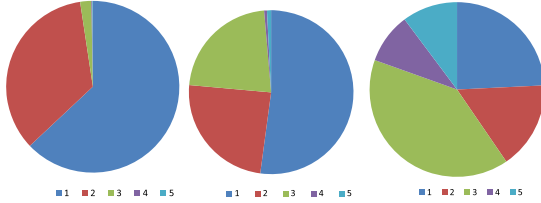
Fig. 2. Percentage share of motor losses at nominal load, at 10, 50, and 350 Hz of supply voltage. 1) Losses in the stator winding. 2) Losses in the rotor winding. 3) Losses in the core (basic and additional). 4) Other additional losses. 5) Mechanical losses [24].

coming from that regulation. The starting structure for the design process was the motor currently used in the washing machine drive. It was a four-pole SK 120/120 motor with a stator outer diameter and a core package length of 120 mm, with stator and rotor with teardrop shape slots and semi-closed rotor slots, with a core made of M470-50A sheet with a thickness of 0.5 mm. Limitations of the motor's overall dimensions, especially its length, were imposed by washing machine manufacturers.

For low values of the supply voltage frequency (10, 20 i 50 Hz), this motor has efficiencies much lower, even than the value required for class IE1 at 50 Hz. To improve the efficiency of the induction machines, it is necessary to analyze the losses' origin. Normally, the losses of an induction motor are classified in five categories: resistive losses in the stator winding; resistive losses in the rotor winding; losses in the core (basic and additional); other additional losses usually referred to as SL and friction and windage losses: mechanical and aerodynamic losses. It should be mentioned that additional core losses are often included in SL, especially when it is difficult to define them correctly.

As presented in [24], at frequencies lower than or equal to the mains frequency 50 Hz, losses in the windings dominate in the motor, while at frequencies significantly higher than the mains' frequency, losses in the motor core dominate (see Fig. 2). Moreover, the motor in the whole range of its operation should achieve the torque's set value on the shaft.

Obtaining the desired values of the electromagnetic torque in a motor with imposed overall dimensions at low frequencies is associated with very high magnetic induction values in the stator and rotor core (exceeding 1.8 T), thus a significant value of the magnetizing current. At the supply voltage frequencies of 10 and 20 Hz, increasing the efficiency would require reducing the windings' resistance, thus reducing the number of series turns of the stator winding and increasing the wire cross-section within the permissible value of the slot filling factor. Despite advances
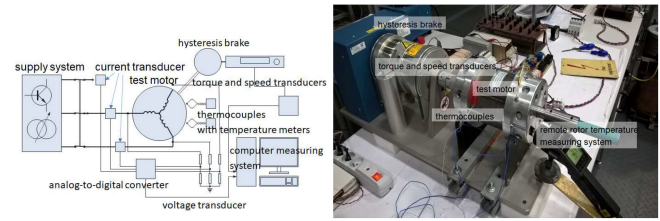
in automation, stator coil windings made by machine are still limited to lower slot fill factors. However, this would cause a further increase in the core's magnetic induction, resulting in a much greater increase in the magnetizing current. Consequently, there is an increase in current in the stator windings and losses in both the core and the motor windings.

An additional difficulty is caused not only by the limitations of the basic dimensions of the core imposed by the washing machine manufacturer, but also by the technological limitations imposed by the motor manufacturer (due to machine winding) and economic considerations, which prevent the use of thinner metal sheets and much lower loss values, which are also much more expensive than the commonly used electrical sheet. Therefore, the development of a modernized motor design meeting the efficiency requirements for at least class IE2 in the entire frequency range of the supply voltage is difficult, requiring a compromise between the various constraints.

III. EXPERIMENTAL SETUP

All measurements were made in the measuring system shown in Fig. 3. The motor was powered either from the mains or from a pulsewidth modulation (PWM) inverter (Mitsubishi FR-D720S-100SC-EC identical to the one used in the washing machine) with a one-phase power supply working with 14.5 kHz PWM switching frequency, and sine evaluated modulation control, 3.8 kVA rated output capacity and 10 A rated current (control methods: V/f control—used; optimum excitation control or general-purpose magnetic flux vector control). The hysteresis braking system Magtrol HD-715-8NA provides precise torque loading independent of shaft speed with the accuracy: $\pm 0.25\%$ (full scale) was used as load. They were measured using precise current transducers and a multichannel analog-to-digital converter of instantaneous currents and voltages (two National Instruments NI-PCI-6133 measuring cards with simultaneous sampling using sampling period 3 μs), as well as rotational speed and load torque. The measurement was controlled by a measuring system running under the control of the LabView program. Based on the measured voltage and current values, the shaft's output power, input power, RMS values of phase voltages, and currents were calculated. The winding resistance was measured after the measurement following IEC 60034-2-1 standard (also IEEE 112) and IEC Std 60034-2-3 [59]. The meters used satisfied the requirements of the above standards including.

Additionally, the temperature of the stator and rotor windings was measured by thermocouples built-in during the model's

construction, with the signal from sensors in the rotor being transmitted wirelessly to the external system. Before taking recordings of each operating point, motor thermal equilibrium was established. An additional element increasing the measurements' accuracy was measuring mechanical losses in a separate system with the tested motor driven by an auxiliary motor and measuring the torque directly on the motor shaft.

IV. IMPROVEMENTS TO THE DESIGN OF A CURRENT MACHINE

The new design of an induction motor to drive an industrial washing machine should reduce both losses in the motor core and its windings. The reduction of losses in the core can be achieved by using a lower thickness of electrical sheet and, as a result, less loss than the commonly used 0.5 mm thick nonoriented sheet, but with slightly worse magnetization characteristics of the sheet. Simultaneously, the sheet used should enable the core to be punched on a mechanical punching machine. Therefore, as shown in works [26], [27], a significant reduction of core losses can be achieved for a 0.2 mm thick sheet. The use of sheets with a smaller thickness, e.g., 0.12 mm or amorphous sheet, as demonstrated in [25],[26], and [29], causes great technological difficulties and requires other ways of cutting out the core, which results in significant damage to both the insulation and structure of these sheets, and, as a result, obtaining losses comparable to 0.2 mm thick sheet. Besides, these sheets have a poorer magnetizability, which especially at low frequencies, when there are significant magnetic induction values in the core, can cause a very high magnetizing current in the motor.

The winding losses can be reduced by reducing the winding resistance, i.e., increasing the cross-sectional area of the stator winding wire, which requires enlarging the stator slots and increasing the rotor slots area. This can be achieved by increasing the stator's outer diameter and enlarging the motor's dimensions within limits permitted by washing machine manufacturers. However, increasing the stator and rotor slots' dimensions cannot reduce the dimensions of the stator teeth or the yoke, as this would further increase the magnetic induction in the motor core and further increase the magnetizing current. The stator resistance can also be reduced by reducing the number of series turns in the stator winding. However, especially at low frequencies, this also causes the magnetic induction to increase excessively.

Taking into account the above considerations, after designing, manufacturing, and testing a dozen or so different motor constructions, a modernized motor structure was finally developed of the SK 135/120 series, with stator drip slots and semiclosed rotor slots with a core made of M270—35A sheet metal with thickness 0.35 mm, the design data of which are given in Table II, meeting the limitations of the overall dimensions imposed by manufacturers of washing machines.

In this table, the design data of the currently produced SK 120/120 motor are presented for comparison. It should be noted that both the number of slots and the stator's internal diameter has been imposed by technological considerations resulting from the use of mechanical manufacturing of the stator windings.

TABLE II
DESIGN DATA FOR MOTOR SK135/120 (IMPROVED CONSTRUCTION) AND FOR CURRENTLY PRODUCED MOTOR SK 120/120

Data	Symbol	Unit	SK135/120	SK120/120
Stator outer diameter	Dse	mm	135	120
Stator inner diameter	Dsi	mm	77	78
Rotor inner diameter	Dri	mm	26	26
Core length	Ls	mm	120	120
Air gap thickness	δ	mm	0.3	0.225
Number of stator slots	Qs	-	24	36
Number of rotor slots	Qr	-	30	32
Number of series turns in the stator winding	Ns	-	100	114
Number of turns in the coil of the stator winding	zsq	-	25	19
Stator winding wire diameter	$dsu1$	mm	0.629	0.53
Stator slot fill factor	$kqs11$	-	0.811	0.755
Stator winding resistance at 20°	$Rs20$	Ω	0.368	0.867
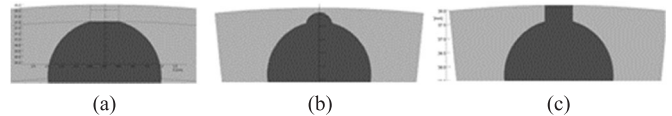
Fig. 4. Rotor slot shape: (a) closed; (b) with reduced thickness bridge and circular undercut; and (c) semiclosed.
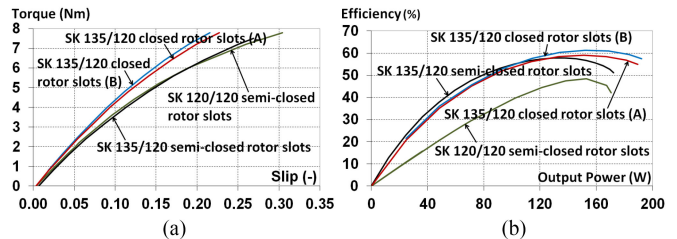
Fig. 5. Measured (a) mechanical and (b) efficiency characteristics at a supply voltage frequency of 10 Hz.
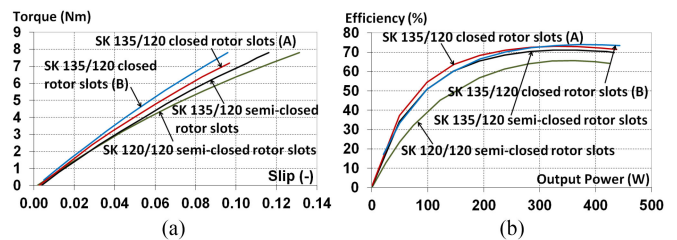
Fig. 6. Measured (a) mechanical and (b) efficiency characteristics at a supply voltage frequency of 20 Hz.

When developing this design, the use of a rotor with closed slots was considered for two different shapes and dimensions of the bridge, shown in Fig. 4.

The measured mechanical and efficiency characteristics of the manufactured SK 120/120 series motor (currently produced) and the designed SK 135/120 series motor with semiclosed and closed rotor slots, for two types of rotor slot bridge, at different values a supply voltage frequency is shown in Figs. 5–7.

After manufacturing and testing of model motors with closed rotor slots and bridge of different thickness, it was found that for low frequencies (10 and 20 Hz), the closure of the rotor
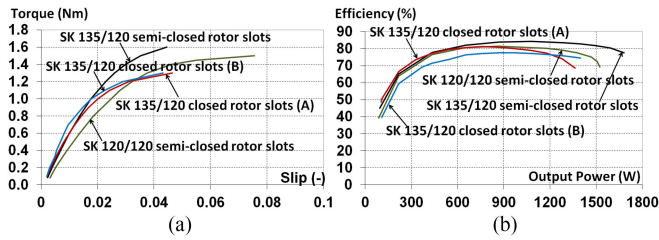
Fig. 7. Measured mechanical and efficiency characteristics at a supply voltage frequency of 350 Hz.

TABLE III
EFFICIENCY OF THE IMPROVED DESIGN MOTOR SK 135/120 AND OF CURRENTLY PRODUCED MOTOR SK 120/120 FOR AN INDUSTRIAL WASHING MACHINE DRIVE

Supply voltage frequency	Output power	Efficiency SK120/120	Efficiency 135/120
Hz	W	%	
10	170	42.1	52.6
20	500	61.5	68.3
50	1500	76.6	82.8
350	1400	76.9	82.8

Fig. 8. Share of higher harmonics in the voltage generated by an exemplary voltage inverter used for investigated washing machine at the fundamental frequency of 350 Hz (left) and 10 Hz (right).

Fig. 9. Harmonic loss components in the stator and rotor core of the SK 135/120 motor, loaded with a torque of 1.16 N·m, when powered by an inverter with a frequency of 350 Hz.

slots improved the mechanical characteristics of the motor and increased its efficiency, especially for the rated load (see Fig. 5 and 6). However, when the motor was supplied with a voltage of 350 Hz, the closing of the rotor slots resulted in a significant reduction of the magnetic induction in the rotor and, as a result, a reduction of the electromagnetic torque of the motor below the permissible value (see Fig. 7), as well as a marked deterioration of efficiency. Based on the measured mechanical and performance characteristics shown in Figs 4–6, the SK 135/120 series motor's design with semi-closed rotor slots was chosen. Much higher efficiency values were obtained for this solution than for the currently produced SK120/120 motor (see Table III). As demonstrates, working in a wide frequency range makes it impossible to take advantage of the solution's positive features with closed rotor slots.

As given in Table III, the efficiency class IE2 was achieved for the SK 135/120 motor when powered with a voltage of 50 and 350 Hz. When this motor was powered with a voltage of 10 Hz, the efficiency was 11.9% lower than for the IE2 class, but at the same time by 10.5% higher than the efficiency of the currently produced motor. In comparison, when the motor was powered with a voltage of 20 Hz, the efficiency obtained is 7.7% lower than for the IE2 class, but at the same time 6.8% higher than the efficiency of the currently produced motor.

V. CALCULATION OF THE CORE LOSSES OF THE MOTOR POWERED BY THE INVERTER FOR THE IMPROVED DESIGN

It can be seen from the above that the exact calculation of the losses in the motor core is crucial for the correct determination of efficiency, especially for higher operating frequencies. It should be noted that the no-load test losses are often directly used when determining the core losses of induction motors. In fact, when the motor is loaded, the basic core losses are somewhat reduced. However, there is an increase in the additional losses caused by the slot and conductive field harmonics, even if the motor is supplied with fundamental harmonic voltage. The power supply from the inverter introduces additional higher harmonics produced by the inverter. Calculating the core losses requires determining the dominant harmonics and calculating the losses considering the core material's properties. The core losses dominate when the motor is running at high frequencies. At the same time, however, in this case, the share of higher harmonics in the voltage generated by the PWM inverter is relatively small. For example, when powered from an exemplary voltage inverter used for investigated washing machine, at the fundamental voltage frequency of 350 Hz, a noticeable role is also played by harmonic five corresponding to the frequency of 1800 Hz, the share of which is 0.23, and harmonic 9, corresponding to the frequency of 3200 Hz, the share of which is 0.233 of the fundamental harmonic (see Fig. 8). The situation is much worse when the motor is supplied with voltage with the fundamental frequency of 10 and 20 Hz (see Fig. 8). Still, in these cases, the share of core losses is minimal, so neglecting additional losses generated by harmonics generated by the inverter has practically no effect on motor losses and efficiency.
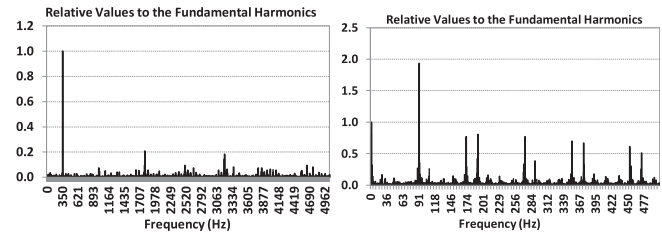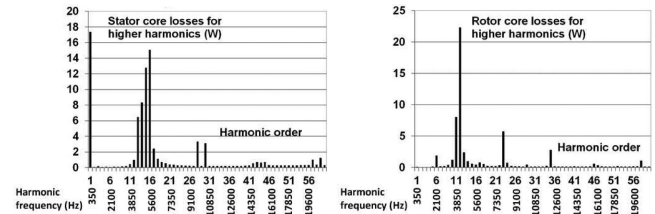
For the designed motor of the SK 135/120 series, calculations of the core losses were performed using the field-circuit model, with the motor being supplied with the basic frequency of 350 Hz, both for the no-load state and the motor load with a torque of 1.16 N·m.

Fig. 9 shows the stator and rotor core losses for higher harmonics (including the losses from the fundamental harmonic in the stator core) as a function of the harmonic order for a motor load of 1.16 N·m. In this case, dominant losses are caused by stator and rotor slots (24 stator slots and 30 rotor slots) with harmonics corresponding to the number of slots or their groups (subharmonics) and multiples of the number of slots. For field-circuit analysis, the commercial software OPERA two-dimensional RM module with the transient eddy-current solver
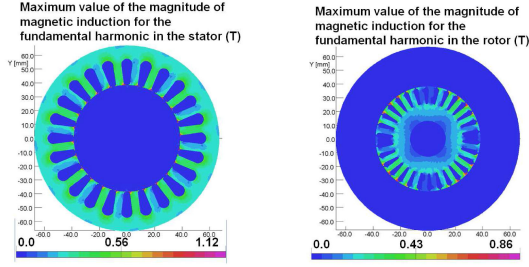
Fig. 10.   Distribution of the maximum value of the magnitude of magnetic induction for the fundamental harmonic in the stator (left) and rotor core (right).
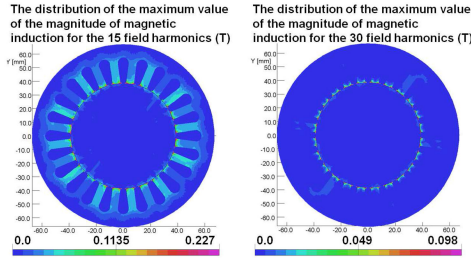
Fig. 11.   Distribution of the maximum value of the magnitude of magnetic induction for the 15 (left) and 30 (right) field harmonics.

was chosen included rotation and a circuit description of the windings with multi-slice modeling of the skewed rotor bars.

Fig. 10(left) shows the distribution of the maximum value of the magnitude of magnetic induction for the fundamental harmonic in the stator core of the SK 135/120 motor, loaded with a torque of 1.16 N·m, with a voltage of 350 Hz. As the motor operates in the field weakening region at 350 Hz, the greater induction value, above 1 T, only occurs in the stator tooth heads. However, the first harmonic induction amplitude's mean value is less than 0.3 T (290 mT). Fig. 10(right) shows the distribution of the maximum value of the magnitude of magnetic induction for the fundamental harmonic for the rotor. This is called the zero harmonic, i.e., the field that rotates synchronously with the rotor at no-load condition and rotates with the rotor at speed resulting from the slip under the load condition. As can be seen, like the stator, higher induction values occur in the heads of the rotor teeth, and the average value is close to the value for the stator.

Fig. 11(left) shows the distribution of the maximum value of the magnitude of magnetic induction for the 15th harmonic of the field in the motor core. This is a typical harmonic resulting from the rotor slotting (30 rotor slots), so its influence mainly occurs in the stator core. As stated previously, this distribution is quite uneven, with a maximum value of 227 mT and an average value of 19.4 mT. This harmonic is concentrated mainly in the heads of the stator teeth, but is also present in the stator teeth, while its presence in the stator yoke is negligible. Fig. 11(right) shows the distribution of the maximum value of the magnitude of magnetic induction for the 30th harmonic of the field in the motor core. It is also the harmonic resulting from the rotor slotting. This distribution is quite uneven, with a maximum value of 9.8 mT and an average value of 4.08 mT, and the harmonic is concentrated mainly in the stator tooth heads.

For this motor, calculations of the core losses were also performed using the analytical method for the same machine operating conditions as for the calculations made using the field-circuit model. The analytical model was based on the equivalent circuit of an induction motor. This model considers the influence of the phenomenon of current displacement on the rotor parameters by the elementary conductors method and the influence of the saturation phenomenon by introducing the saturation factor depending on the resultant flow in the stator and rotor windings. The basic losses in the stator teeth were calculated for the fundamental harmonic of the field, when the tooth was divided along with the height into four layers, as the sum of the losses in each layer for the actual value of the induction occurring in this layer, while the basic losses in the stator yoke were calculated for the mean value of the induction in the yoke.

In the analytical calculation of the additional core losses, the higher harmonics of the air gap's magnetic fields were included. In [24], additional surface losses in the stator and rotor teeth ($P^{\text{surf}}_{s(r),\nu_{r(s)}}$), caused by the stator (rotor) flux density $B_{r(s),\nu r(s)}$ harmonics of rank $\nu_{s(r)}$, were calculated using the method from [26], based on the measured specific core losses w_{Fe} for all individual harmonics of the stator and the rotor fields (in the frequency range from 10 to 14400 Hz). In this method, concerning the formulas provided in [26], the dependence specifying the depth of field penetration into the heads of the stator and rotor teeth ($\lambda_{s(r),\nu r(s)}$ (m)) was modified, according to [53]

$$P^{\text{surf}}_{s(r),\nu_{r(s)}} = w_{\text{Fe}}\left(B_{r(s)}, \nu_{r(s)}, f_{\nu r(s)}\right) \rho_{\text{Fe}} S_{s(r)}\lambda_{s(r)}, \nu_{r(s)}$$

$$S_{s(r)} = \pi \leftrightarrows D_{si(re)}k_{t_{s(r)}}L_{s(r)}k_{\text{Fe}}$$

$$k_{t_{s(r)}} = \frac{t_{s(r)} - b_{s(r)}}{t_{s(r)}}; \; \lambda_{s(r),\nu_{r(s)}} = \frac{D_{si(re)}f_s}{2p\left|f_{\nu_{r(s)}} - f_s\right| \leftrightarrows}f_{\nu_{r(s)}}$$

$$= f_s\left|1 + \frac{\nu_{r(s)} - p}{p}\right|; \; t_{s(r)} = \frac{\pi D_{si(re)}}{Q_{s(r)}} \quad (1)$$

where w_{Fe} (W/kg) is the specific iron losses for $f\nu_{r(s)}$ and $Br(s),\nu r(s)$, ρ_{Fe} (kg/m^3) is the mass density of the core material, $D_{si(re)}$ (m) is the internal (external) diameter of the stator (rotor) core, $L_{s(r)}$ (m) is the length of stator (rotor) core, k_{Fe} is the packing factor of the core, $t_{s(r)}$ (m) is the stator (rotor) slot pitch, $b_{s(r)}$ (m) is the width of the stator (rotor) slot opening, $Q_{s(r)}$ is the number of stator (rotor) slots, f_s (Hz) is the frequency of the first harmonic stator field, and p is the number of pole pairs.

Total additional surface losses in the stator or rotor teeth were calculated from the formula [26]

$$P^{\text{surf}}_{s(r)} = \sum_{\nu_{r(s)}} P^{\text{surf}}_{s(r),\nu_{r(s)}}. \quad (2)$$

Additional pulsation losses in the stator teeth P^{puls}_s, caused by the harmonic rotor fields, were calculated using the formula in the form given in [26].

TABLE IV

CALCULATION RESULTS FOR THE MOTOR LOAD CONDITION OF THE SK 135/120 MOTOR WITH A TORQUE OF 1.16 N·M, WITH THE SUPPLY OF THE FUNDAMENTAL VOLTAGE HARMONIC WITH A FREQUENCY OF 350 Hz

	Torque	Input power	Output power	Speed	Stator current	Total core losses
	Nm	W	W	rpm	A	W
analytical model	1.16	1488	1255	10331	4.53	113.1
field-circuit model	1.16	1500	1244	10156	4.63	115.5
measurements	1.16	1492	1248	10270	4.69	116.0

TABLE V

CALCULATION RESULTS OF INDIVIDUAL COMPONENTS OF THE CORE LOSSES FOR THE MOTOR LOAD CONDITION SK 135/120 WITH A TORQUE OF 1.16 N·M, WITH THE SUPPLY OF THE FUNDAMENTAL VOLTAGE HARMONIC WITH A FREQUENCY OF 350 Hz

Model	Basic core losses P_c	Additional core losses in stator P_{cdds}	Total core losses in stator	Additional core losses in rotor P_{cdds}	Total core losses sP_c
	(W)	(W)	(W)	(W)	(W)
analytical	18.58	47.48	66.06	47.02	113.08
field-circuit	17.32	52.66	69.98	45.50	115.48

TABLE VI

RESULTS OF CALCULATING LOSSES IN THE CORE FOR THE MOTOR LOAD CONDITION SK 135/120 WITH A TORQUE OF 7.8 N·M. WHEN SUPPLIED FROM AN INVERTER WITH VOLTAGE WITH A FUNDAMENTAL HARMONIC FREQUENCY OF 10 Hz

	Core losses due to the fundamental voltage harmonic	Core losses due to higher voltage harmonics				Total core losses
		9	17	19	27	
	W	W	W	W	W	W
Analytical model	4.90	6.56	1.01	1.19	0.79	14.45
Measurements	-	-				14.94

Fig. 12. Measured (solid line) and calculated (dashed line) loss characteristics of the SK 135/120 motor; friction and ventilation losses, components of losses and total losses at supply frequency 10, 20, and 350 Hz.

Total core losses were calculated as the sum of basic losses and additional surface and pulsation losses in the stator core and additional surface losses in the rotor core.

The results of calculating the losses in the core with the use of the field-circuit model and obtained from the analytical formulas taking into account the higher harmonics generated in the motor while supplying the fundamental voltage harmonics are given in Table IV that shows a comparison of the calculation results for the motor load condition, obtained by the field-field and analytical method, for the same value of the motor load torque. The rotational speeds are slightly different. Hence, there are differences in the calculated loss values. It should be noted that although the calculations are performed with the omission of higher harmonics generated by the inverter, the calculation results obtained both by the circuit method and the analytical method are very similar to the measurement results, which is confirmed by the fact that in this case, the influence of higher harmonics generated by the inverter is very slight.

The calculation results of the individual components of the core losses made using the field-circuit model and obtained from the analytical formulas considering the higher harmonics generated in the motor while supplying the fundamental voltage harmonics are given in Table V.

The situation is different when the motor is supplied with a voltage of 10 or 20 Hz. Under these conditions, very high induction values occur in the motor, especially significant saturation of the heads of the stator and rotor teeth due to the main flux effect and the leakage fluxes generated by the currents flowing in the stator and rotor windings.

The calculation results of the individual components of the core losses obtained from the analytical formulas considering the dominant higher harmonics generated in the motor while supplying from PWM are given in Table VI.

VI. POSSIBILITIES OF INCREASING THE EFFICIENCY OF THE SK 135/120 MOTOR

To analyze the possibility of increasing the efficiency of the designed SK 135/120 motor, especially at low frequencies of the supply voltage, the analysis of individual components of losses occurring in this motor under load conditions was performed. Fig. 12 shows the mechanical losses of the motor and the total losses and their individual components occurring when the motor is supplied with the voltage of 10, 20, and 350 Hz.

As can be seen from Fig. 12, at the frequency of the supply voltage of 10 and 20 Hz, losses in the stator winding dominate, that even at no-load operation reach a significant value, due to the high value of the magnetizing current and, consequently, the high value of total current in the motor windings. This is due to very high magnetic induction values in the motor core. It is impossible to reduce losses in windings by using a wire with a larger cross-section due to the limitation of the stator slot filling factor and the limited possibility of increasing the rotor slot cross-section. The core losses are much smaller for these operating states. It should be noted, however, that the basic losses in the core for these frequencies amount to 20%–30% of the total losses in the core and decrease with increasing motor load, while the remaining part consists of additional losses - pulsation and surface, increasing with increasing current in the machine windings.
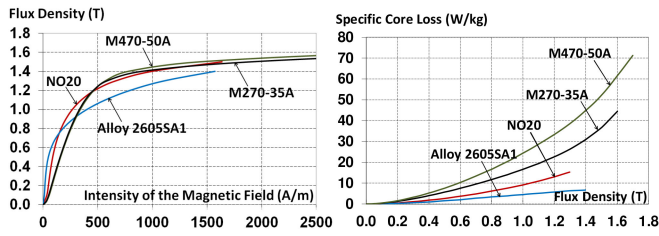
Fig. 13. Measured magnetization characteristics and specific loss characteristics at 300 Hz, for four types of electrical sheet.

At the supply voltage frequency of 350 Hz, despite the low value of the magnetic induction in the motor core, the losses in the core are greater than the sum of the losses in the stator and rotor windings, with the basic losses at no-load running at 70% of the total losses in the core. In contrast, at the motor load, they decrease to 15% of total core losses. In this case, reducing these losses can only be achieved by applying a magnetic material with a lower loss to the motor core.

Due to the design and technological limitations imposed by motor manufacturers, as well as the need to obtain the required value of the electromagnetic torque, especially at 350 Hz and very high core saturation at low frequencies (10 and 20 Hz), reduction of winding losses by reducing the number of series turns of the stator winding and the use of larger diameter wires is practically impossible. A reduction in winding losses could also be achieved by reducing the core induction and the magnetizing current, and hence also the current in the motor windings, by increasing the number of turns in the stator winding, provided that the increase in losses due to the increase in winding resistance would be less than the reduction in losses due to the reduction current, but this, in turn, would make it impossible to obtain the required value of electromagnetic moment at a frequency of 350 Hz. Therefore, a further improvement in the motor's efficiency, in this case, would only be possible by reducing the core losses.

For this purpose two types of sheets were considered: NO20 produced by Swedish company Cogent Surahammars Bruks AB, and for comparison, amorphous steel Alloy 2605SA1 (manufactured by METGLAS), which, as shown in [29], allows us to obtain a significant increase in the efficiency of the motor. Fig. 13 shows the measured magnetization and specific loss characteristics (for an example of the supply voltage frequency 300 Hz) of the M270-35A electrical sheet with a thickness of 0.35 mm, of which the SK 135/120 motor core was made, and the M470-50A sheet with a thickness of 0.5 mm, from which the core of the currently produced motor was made, and for comparison, sheets of lower loss: NO20 with the thickness of 0.2 mm, and amorphous steel Alloy 2605SA1 with the thickness of 0.0254 mm.

Both the NO20 sheet and the amorphous sheet have a worse magnetization curve than the M270-35A and M470-50A sheets, while much better specific losses than these sheets.

Figs. 14–16 show the calculated mechanical characteristics, current in the stator winding, total losses, and motor efficiency 135/120 as a function of load for motors with a core made of various types of metal sheets, at frequencies of 10, 20, and 350 Hz.
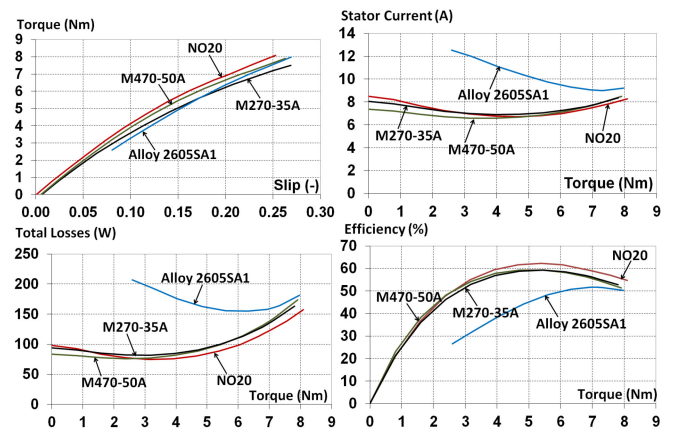
Fig. 14. Calculated mechanical characteristics, current in the stator winding, total losses, and efficiency as a function of the torque on the shaft of the motor with a core made of various types of electrical sheet at a supply voltage frequency of 10 Hz.
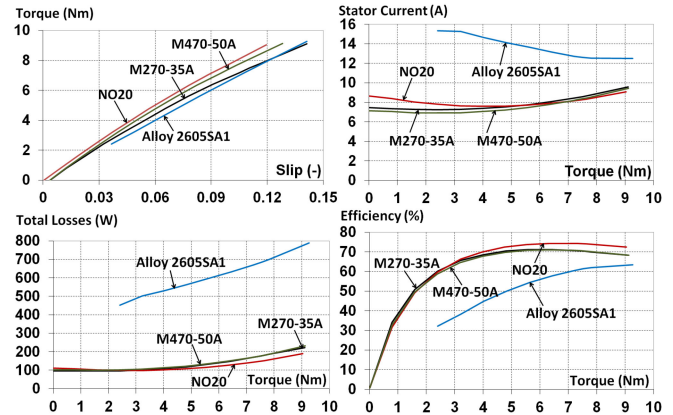
Fig. 15. Calculated mechanical characteristics, current in the stator winding, total losses, and efficiency as a function of the torque on the shaft of the motor with a core made of various types of electrical sheet at a supply voltage frequency of 20 Hz.
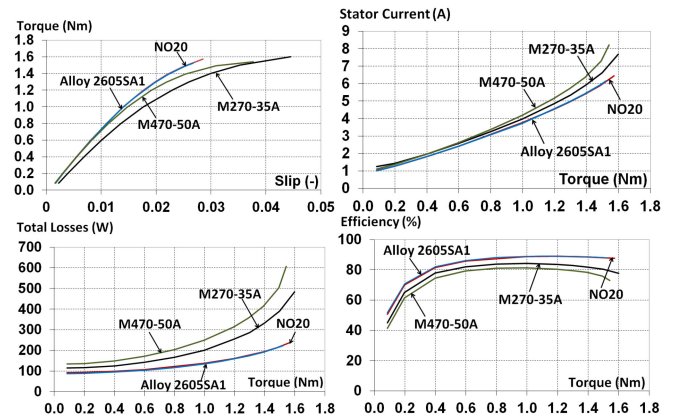
Fig. 16. Calculated mechanical characteristics, current in the stator winding, total losses, and efficiency as a function of the torque on the shaft of the motor with a core made of various types of electrical sheet at a supply voltage frequency of 350 Hz.

TABLE VII
EFFICIENCY OF THE IMPROVED DESIGN MOTOR SK 135/120 WITH A CORE MADE OF M270-35A AND NO20 SHEET

Frequency of supply voltage	Output power	Efficiency M270-35A	Efficiency NO20	Efficiency class
Hz	W	%	%	
10	170	52.6	60,0	IE1
20	500	68.3	72,6	IE1
350	1400	82.8	88,8	IE4

As can be seen from Figs. 14–16, the amorphous sheet has the lowest specific losses, but at the same time the worst magnetization characteristics. Therefore, in the motor at low frequencies of the supply voltage, when there are very high induction values in the core (exceeding 1.8 T at no-load), the magnetizing current reaches very high values. This causes a strong increase in the stator winding currents and a considerable increase in the motor windings' losses, significantly outweighing the reduction of losses in the motor core. On the other hand, when the motor is operating at the frequency of the supply voltage of 350 Hz, the induction in the core does not exceed 0.5 T, so the work takes place practically on the linear part of the characteristic. In this case, the use of an amorphous sheet is advantageous. It should be emphasized, however, that the smaller the thickness of the sheet, the lower the core iron filling factor (for sheet M470-50A-0.96-0.97, for sheet M270 -35A - 0.94, for sheet NO20 - 0.93, while for amorphous sheet Alloy 2605SA1 - 0.86). Therefore, the motor's characteristics with a core made of amorphous sheet practically coincide in this case with the characteristics of the motor with a core made of NO20. Also, the technology of cutting NO20 cores with a thickness of 0.2 mm is practically the same as for electrical sheets with a thickness of 0.5 or 0.35 mm, and the only barrier to its use are economic considerations because this sheet is almost twice as expensive as 0.5 or 0.35 mm thick sheet metal. However, the use of NO20 for the motor core allows for a significant increase in the efficiency of the motor in the entire frequency range of its operation and achieving, even for frequencies of 10 and 20 Hz, the efficiency class IE1 (see Table VII) specified for the motor operating at the mains frequency.

VII. CONCLUSION

Obtaining high efficiency for a motor operating in a wide frequency range while maintaining the required electromagnetic torque value was much more difficult than for a motor operating at a constant frequency voltage. Increasing efficiency at low operating frequencies requires limiting both losses and current in the motor windings, which was generally only achievable by increasing the motor's dimensions, often not possible due to limitations in the driven equipment. Increasing the efficiency was achieved by changing the rotor cage material from aluminum to copper, but this requires a change of technology at the manufacturer. Increasing the value of the voltage supplying the motor at low frequencies while maintaining a constant value of induction, i.e., what was associated with an increase in the number of series turns of the stator winding, causes a decrease in the current of the windings. However, reducing losses in

the windings will be achieved only if the resistance does not increase significantly. Moreover, it is associated with a field weakening when the motor was supplied with a voltage of many times greater frequency. It was impossible to obtain the required electromagnetic torque value in such a motor. Therefore, when designing motors operating in a wide frequency range, it was necessary to consider all these aspects and select both the optimal dimensions of the magnetic circuit and the number of series turns of the stator winding and appropriate voltage control of the inverter at low frequencies. Also, satisfactory results was obtained by using a core material with as little specific losses as possible, but at the same time with good magnetizability. However, when selecting such a material, both technological and economic aspects should be taken into account.

To summarize, the main achievements are as follows.
1) Refinement of the method of calculating additional surface losses in the core.
2) Demonstration of the main problems in the design of energy-saving induction motors operating in a wide frequency range (35:1 or 35:2) and a compromise approach in solving contradictory conditions.
3) Development of a motor structure achieves high efficiency (falling into efficiency classes. specified for 50 Hz) in a wide frequency range, considering the imposed quite restrictive design constraints, technological factors, and material costs, allowing for effective competition demanding market.

REFERENCES

[1] G. Bramerdorfer, J. A. Tapia, J. J. Pyrhönen, and A. Cavagnino, "Modern electrical machine design optimization: Techniques, trends, and best practices," *IEEE Trans. Ind. Electron.*, vol. 65, no. 10, pp. 7672–7684, Oct. 2018, doi: 10.1109/TIE.2018.2801805.

[2] D. Zhang, H. Dai, H. Zhao, and T. Wu, "A fast identification method for rotor flux density harmonics and resulting rotor iron losses of inverter-fed induction motors," *IEEE Trans. Ind. Electron.*, vol. 65, no. 7, pp. 5384–5394, Jul. 2018, doi: 10.1109/TIE.2017.2779432.

[3] A. T. de Almeida, F. J. T. E. Ferreira, and G. Baoming, "Beyond induction motors—Technology trends to move up efficiency," *IEEE Trans. Ind. Appl.*, vol. 50, no. 3, pp. 2103–2114, May/Jun. 2014, doi: 10.1109/TIA.2013.2288425.

[4] J. Rivera Dominguez, C. Mora-Soto, S. Ortega-Cisneros, J. J. Raygoza Panduro, and A. G. Loukianov, "Copper and core loss minimization for induction motors using high-order sliding-mode control," *IEEE Trans. Ind. Electron.*, vol. 59, no. 7, pp. 2877–2889, Jul. 2012, doi: 10.1109/TIE.2011.2171170.

[5] S. Di Gennaro, J. Rivera Domínguez, and M. A. Meza, "Sensorless high order sliding mode control of induction motors with core loss," *IEEE Trans. Ind. Electron.*, vol. 61, no. 6, pp. 2678–2689, Jun. 2014, doi: 10.1109/TIE.2013.2276311.

[6] A. M. Bazzi and P. T. Krein, "Review of methods for real-time loss minimization in induction machines," *IEEE Trans. Ind. Appl.*, vol. 46, no. 6, pp. 2319–2328, Nov./Dec. 2010, doi: 10.1109/TIA.2010.2070475.

[7] L. Aarniovuori, M. Niemelä, J. Pyrhönen, W. Cao, and E. B. Agamloh, "Loss components and performance of modern induction motors," in *Proc. 13th Int. Conf. Elect. Mach.*, 2018, pp. 1253–1259.

[8] A. Boglietti, A. Cavagnino, L. Ferraris, and M. Lazzari, "Induction motor equivalent circuit including the stray load losses in the machine power balance," *IEEE Trans. Energy Convers.*, vol. 23, no. 3, pp. 796–803, Sep. 2008, doi: 10.1109/TEC.2008.921467.

[9] M. Aminu, J. Mushenya, P. S. Barendse, and M. A. Khan, "Converter-fed induction motor efficiency measurement under variable frequency/load points: An extension of the IEC/TS 60034-2-3," in *Proc. IEEE Energy Convers. Congr. Expo.*, 2019, pp. 3046–3052, doi: 10.1109/ECCE.2019.8912619.

[10] A. Boglietti, R. Bojoi, A. Cavagnino, and S. Vaschetto, "Influence of the sinusoidal supply frequency on the induction motor stray load losses," in *Proc. 38th Annu. Conf. IEEE Ind. Electron. Soc.*, 2012, pp. 1847–1851, doi: 10.1109/IECON.2012.6388920.

[11] C. Choudhury, and N. K. Deshmukh, "A novel method for reduction of stray loss in induction motor," in *Proc. IEEE Power Energy Conf. Illinois*, 2013, pp. 101–105, doi: 10.1109/PECI.2013.6506042.

[12] A. A. Jimoh, R. D. Findlay, and M. Poloujadoff, "Stray losses in induction machines: Part i, definition, origin and measurement," *IEEE Trans. Power App. Syst.*, vol. PAS-104, no. 6, pp. 1500–1505, Jun. 1985, doi: 10.1109/TPAS.1985.319165.

[13] K. K. Schwarz, "Survey of basic stray losses in squirrel-cage induction motors," *Proc. Inst. Elect. Eng.*, vol. 111, pp. 1565–1574, 1964.

[14] H. Nishizawa, K. Itomi, S. Hibino, and F. Ishibashi, "Study on reliable reduction of stray load losses in three-phase induction motor for mass production," *IEEE Trans. Energy Convers.*, vol. EC-2, no. 3, pp. 489–495, Sep. 1987, doi: 10.1109/TEC.1987.4765877.

[15] M. Aminu, J. Mushenya, P. S. Barendse, and M. A. Khan, "Converter-fed induction motor efficiency measurement under variable frequency/load points: An extension of the IEC/TS 60034-2-3," in *Proc. IEEE Energy Convers. Congr. Expo.*, 2019, pp. 3046–3052, doi: 10.1109/ECCE.2019.8912619.

[16] S. Vaschetto, A. Cavagnino, E. B. Agamloh, and A. Tenconi, "Enhanced stray-load loss measurements through a zigzag variable load test approach," *IEEE Trans. Ind. Appl.*, vol. 57, no. 1, pp. 226–235, Jan./Feb. 2021, doi :10.1109/TIA.2020.3029757.

[17] P. Pillay, M. Al-Badri, P. Angers, and C. Desai, "A new stray-load loss formula for small and medium-sized induction motors," *IEEE Trans. Energy Convers.*, vol. 31, no. 3, pp. 1221–1227, Sep. 2016, doi: 10.1109/TEC.2016.2539959.

[18] E. B. Agamloh, "An evaluation of induction machine stray load loss from collated test results," *IEEE Trans. Ind. Appl.*, vol. 46, no. 6, pp. 2311–2318, Nov./Dec. 2010, doi: 10.1109/TIA.2010.2070474.

[19] A. Boglietti, A. Cavagnino, L. Ferraris, and M. Lazzari, "Induction motor equivalent circuit including the stray load losses in the machine power balance," *IEEE Trans. Energy Convers.*, vol. 23, no. 3, pp. 796–803, Sep. 2008, doi: 10.1109/TEC.2008.921467.

[20] R. Kumar, P. Kumar, T. Kanekawa, and K. Oishi, "Stray loss model for induction motors with using equivalent circuit parameters," *IEEE Trans. Energy Convers.*, vol. 35, no. 2, pp. 1036–1045, Jun. 2020, doi: 10.1109/TEC.2020.2964616.

[21] M. Ghasemi Bijan and P. Pillay, "Induction machine efficiency evaluation using the finite element analysis software and a new mechanical loss formula," in *Proc. IEEE Int. Electric Mach. Drives Conf.*, 2019, pp. 301–306, doi: 10.1109/IEMDC.2019.8785189.

[22] E. Dlala and A. Arkkio, "A general model for investigating the effects of the frequency converter on the magnetic iron losses of a squirrel-cage induction motor," *IEEE Trans. Magn.*, vol. 45, no. 9, pp. 3303–3315, Sep. 2009, doi: 10.1109/TMAG.2009.2021066.

[23] D. Zhang, H. Zhao, and T. Wu, "The rotor copper and iron loss analysis of inverter-fed induction motor considering rotor slip frequency," in *Proc. IEEE Energy Convers. Congr. Expo.*, 2017, pp. 2412–2419, doi: 10.1109/ECCE.2017.8096465.

[24] M. Dems, K. Komeza, and K. Majer, "Core losses of the induction motor operating in a wide frequency range supplied from the inverter," *Int. J. Appl. Electromagn. Mech.*, vol. 64, pp. 1–18, 2020.

[25] M. Dems, K. Komeza, and H. G. Rodríguez, "Methods for increasing the efficiency of an asynchronous motor with increased speed fed from the PWM inverter," *Int. J. Appl. Electromagn. Mech.*, vol. 57, no. S1, pp. 61–71, 2018.

[26] M. Dems and K. Komeza, "The influence of electrical sheet on the core losses at no-load and full-load of small power induction motors," *IEEE Trans. Ind. Electron.*, vol. 64, no. 3, pp. 2433–2442, Mar. 2017, doi: 10.1109/TIE.2016.2587817.

[27] M. Dems and K. Komeza, "Performance characteristics of a high-speed energy-saving induction motor with an amorphous stator core," *IEEE Trans. Ind. Electron.*, vol. 61, no. 6, pp. 3046–3055, Jun. 2014, doi: 10.1109/TIE.2013.2251739.

[28] M. Dems and K. Komeza, "Finite element and analytical calculations of no-load core losses in energy-saving induction motors," *IEEE Trans. Ind. Electron.*, vol. 59, no. 7, pp. 2934–2946, Jul. 2012, doi: 10.1109/TIE.2011.2168795

[29] M. Dems, K. Komeza, S. Wiak, T. Stec, and M. Kikosicki, "Application of circuit and field-circuit methods in designing process of small induction motors with stator cores made from amorphous iron," *Int. J. Comput. Math. Elect. Electron. Eng.*, vol. 25, no. 2, pp. 283–296, 2006.

[30] M. Ojaghi and S. Nasiri, "Modeling eccentric squirrel-cage induction motors with slotting effect and saturable teeth reluctances," *IEEE Trans. Energy Convers.*, vol. 29, no. 3, pp. 619–627, Sep. 2014, doi: 10.1109/TEC.2014.2320823.

[31] Q. Gu, L. Yuan, Z. Zhao, F. Liu, and J. Sun, "An accurate stray loss calculation method of squirrel-cage induction motors for efficiency optimization," in *Proc. 18th Int. Conf. Elect. Mach. Syst.*, 2015, pp. 143–149.

[32] H. Gorginpour, H. Oraee, and E. Abdi, "Calculation of core and stray load losses in brushless doubly fed induction generators," *IEEE Trans. Ind. Electron.*, vol. 61, no. 7, pp. 3167–3177, Jul. 2014, doi: 10.1109/TIE.2013.2279357.

[33] B. Heller and V. Hamata, *Harmonics Field Effects in Induction Machines*. New York, NY, USA: Elsevier Scientific Pub., 1977.

[34] T. Knopik and A. Binder, "Measurement proven analytical and numerical models for calculation of the teeth flux pulsations and harmonic torques of skewed squirrel cage induction machines," in *Proc. IEEE Energy Convers. Congr. Expo.*, 2011, pp. 162–169, doi 10.1109/ECCE.2011.6063764.

[35] P. L. Alger, *Induction Machines*, New York, NY, USA: Gordon and Beach, 1970.

[36] E. B. Agamloh, "An evaluation of induction machine stray load loss from collated test results," *IEEE Trans. Ind. Appl.*, vol. 46, no. 6, pp. 2311–2318, Jan. 2011.

[37] P. L. Alger, G. Angst, and E. J. Davies, "Stray-load losses in polyphase induction machines," *IEEE Trans. Power Appl. Syst.*, vol. 78, no. 3, pp. 349–355, Jun. 1959, doi:10.1109/T-AIEE.1934.5056621.

[38] B. Piepenbreier and F. Taegen, "Surface losses in cage induction motors," in *Proc. Beijing Int. Conf. Elect. Mach.*, 1987, pp. 326–329.

[39] T. Sliwinski, *The Methods of the Induction Motors Calculation*. Warszawa, Poland: PWN, 2008.

[40] S. Williamson and C. I. McClay, "Optimization of the geometry of closed rotor slots for cage induction motors," *IEEE Trans. Ind. Appl.*, vol. 32, no. 3, pp. 560–568, May/Jun. 1996, doi: 10.1109/28.502167.

[41] M. P. Magill and P. T. Krein, "Examination of design strategies for inverter-driven induction machines," in *Proc. IEEE Power Energy Conf. Illinois*, 2012, pp. 1–6, doi: 10.1109/PECI.2012.618458.

[42] F. G. G. D. Buck, "Design adaptation of inverter-supplied induction motors," *IEEE J. Elect. Power Appl.*, vol. 1, no. 2, pp. 54–60, May 1978, doi: 10.1049/ij-epa.1978.0010.

[43] C. Shumei, D. Ying, and S. Liwei, "Rotor slots design of induction machine for hybrid electric vehicle drives," in *Proc. IEEE Veh. Power Propulsion Conf.*, 2006, pp. 1–3, doi: 10.1109/VPPC.2006.364375.

[44] M. Amrhein and P. T. Krein, "Rotor designs for small inverter-dedicated induction machines," in *Proc. IEEE Int. Elect. Mach. Drives Conf.*, 2003, vol. 2, pp. 1279–1285, 2003, doi: 10.1109/IEMDC.2003.1210404.

[45] Z. M. Zhao, S. Meng, C. C. Chan, and E. W. C. Lo, "A novel induction machine design suitable for inverter-driven variable speed systems," *IEEE Trans. Energy Convers.*, vol. 15, no. 4, pp. 413–420, Dec. 2000, doi: 10.1109/60.900502.

[46] M. Kondo, R. Ebizuka, and A. Yasunaga, "Rotor design for high efficiency induction motors for railway vehicle traction," in *Proc. Int. Conf. Elect. Mach. Syst.*, 2009, pp. 1–4, doi: 10.1109/ICEMS.2009.5382961.

[47] H. Li, and K. W. Klontz, "Rotor design to reduce secondary winding harmonic loss for induction motor in hybrid electric vehicle application," in *Proc. IEEE Energy Convers. Congr. Expo.*, 2016, pp. 1–6, doi: 10.1109/ECCE.2016.7855411.

[48] N. Kunihiro, K. Nishihama, M. Iizuka, K. Sugimoto, and M. Sawahata, "Investigation into loss reduced rotor slot structure by analyzing local behaviors of harmonic magnetic fluxes in inverter-fed induction motor," *IEEE Trans. Ind. Appl.*, vol. 53, no. 2, pp. 1070–1077, Mar./Apr. 2017, doi: 10.1109/TIA.2016.2642481.

[49] D. G. Kokalj, "Variable frequency drives for commercial laundry machines," *IEEE Ind. Appl. Mag.*, vol. 3, no. 3, pp. 27–30, May/Jun. 1997, doi: 10.1109/2943.589889.

[50] "Laying down ecodesign requirements for electric motors variable speed drives pursuant to Directive 2009/125/EC Eur. Parliament Council, amending Regulation (EC) No 641/2009 with regard to ecodesign requirements for glandless standalone circulators glandless circulators Integrated products repealing Commission Regulation (EC) No 640/2009," *ELI*, Oct. 2019, [Online]. Available: http://data.europa.eu/eli/reg/2019/1781/oj

[51] L. Alberti and D. Troncon, "Design of electric motors and power drive systems according to efficiency standards," *IEEE Trans. Ind. Electron.*, to be published, doi: 10.1109/TIE.2020.3020028.

[52] Rotating Electrical Machines - Part 2-3: Specific Test Methods for Determining Losses and Efficiency Of Converter-Fed AC Motors, IEC Std 60034-2-3, Mar. 2020.

[53] H. B. Ertan, K. Leblebicioglu, B. Avenoglu, and M. Pirgaip, "High-Frequency loss calculation in a smooth rotor induction motor using FEM," *IEEE Trans. Energy Convers.*, vol. 22, no. 3, pp. 566–575, Sep. 2007, doi: 10.1109/TEC.2006.881079.

Krzysztof Komeza (Senior Member, IEEE) received the Ph.D. degree in 1983 and the D.Sc. degree in 1995 from the Technical University of Lodz, Lodz, Poland.

He is currently a Professor of Institute of Mechatronics and Information Systems, Technical University of Lodz. From 1998, he was a Professor with the Technical University of Lodz. He has done a number of consultancy works for electrical machines industry. He has authored or coauthored more than 210 papers. His research interests include computational electromagnetics, efficient finite-element computations and coupled field computations and design, and optimization of electrical machines.

Maria Dems (Member, IEEE) received the Ph.D. degree in 1978, respectively, the D.Sc. degree in 1996 and title Prof. in 2012.

From 1998, she has a Professor with the Technical University of Lodz, Lodz, Poland. She is an author or joint author of over 180 publications. She has done a lot of consultancy work for electrical machines industry. She specializes in electrical engineering, especially in modeling, design and optimization of electrical machines, and applications of modern tools, databases, and expert systems.